Biochimica et Biophysica Acta 1797 (2010) 222–232

Contents lists available at ScienceDirect

Biochimica et Biophysica Acta

journal homepage: www.elsevier.com/locate/bbabio

Structural characterization of a family of cytochromes c_7 involved in Fe(III) respiration by *Geobacter sulfurreducens*

P.R. Pokkuluri, Y.Y. Londer [1], X. Yang, N.E.C. Duke, J. Erickson, V. Orshonsky, G. Johnson, M. Schiffer *

Biosciences Division, Argonne National Laboratory, Argonne, IL 60439, USA

ARTICLE INFO

Article history:
Received 30 July 2009
Received in revised form 16 October 2009
Accepted 20 October 2009
Available online 24 October 2009

Keywords:
Cytochrome c_7 structure
Heme-puckering
Multiheme cytochrome
Electron transfer
Fe(III) reduction
Geobacter sulfurreducens

ABSTRACT

Periplasmic cytochromes c_7 are important in electron transfer pathway(s) in Fe(III) respiration by *Geobacter sulfurreducens*. The genome of *G. sulfurreducens* encodes a family of five 10-kDa, three-heme cytochromes c_7. The sequence identity between the five proteins (designated PpcA, PpcB, PpcC, PpcD, and PpcE) varies between 45% and 77%. Here, we report the high-resolution structures of PpcC, PpcD, and PpcE determined by X-ray diffraction. This new information made it possible to compare the sequences and structures of the entire family. The triheme cores are largely conserved but are not identical. We observed changes, due to different crystal packing, in the relative positions of the hemes between two molecules in the crystal. The overall protein fold of the cytochromes is similar. The structure of PpcD differs most from that of the other homologs, which is not obvious from the sequence comparisons of the family. Interestingly, PpcD is the only cytochrome c_7 within the family that has higher abundance when *G. sulfurreducens* is grown on insoluble Fe (III) oxide compared to ferric citrate. The structures have the highest degree of conservation around "heme IV"; the protein surface around this heme is positively charged in all of the proteins, and therefore all cytochromes c_7 could interact with similar molecules involving this region. The structures and surface characteristics of the proteins near the other two hemes, "heme I" and "heme III", differ within the family. The above observations suggest that each of the five cytochromes c_7 could interact with its own redox partner via an interface involving the regions of heme I and/or heme III; this provides a possible rationalization for the existence of five similar proteins in *G. sulfurreducens*.

© 2009 Elsevier B.V. All rights reserved.

1. Introduction

The bacteria belonging to the Geobacteraceae family thrive in subsurface environments where dissimilatory Fe(III) reduction is dominant. These organisms possess properties of interest in the development of bioremediation tools [1-3] and in their use in biofuel cells [4-6]. *Geobacter sulfurreducens* (*Gs*), with its genome fully sequenced [7] and a genetic system available [8], serves as a model organism for the Geobacteraceae. The organism *Gs* has the ability to oxidize organic compounds, with Fe(III) or other metal ions (or metal oxides) such as U(VI) serving as electron acceptors. The genome of *Gs* encodes a large number of *c*-type cytochromes that carry out various electron transfer functions in the versatile respiratory pathways of the organism. Of the 111 cytochromes predicted by the genome, 91 were identified as being produced in one of the various growth conditions tested [9]. Multiheme cytochromes have been implicated in the electron transport chain(s) used by the organism in the reduction of soluble Fe(III) (ferric citrate) or insoluble Fe(III) oxides, as well as in transfer of electrons to electrodes [10-12]. In addition, the cytochromes may serve as capacitors (electron storage sinks) that for brief moments allow electron flow from the inner membrane to the periplasm in the absence of suitable electron acceptors. Such an electron storage capability would allow *Geobacter* species to move toward zones where electron acceptors are available, as suggested by Nunez and co-workers [13].

Small periplasmic cytochromes c_3 (tetraheme; about 110–120 amino acids) have been well studied in various organisms belonging to the Desulfovibrio family of the δ-proteobacteria. The cytochromes c_7 (triheme; about 70 amino acids) are structurally homologous to the cytochromes c_3. Several structures of cytochromes c_3 from the Desulfovibrio family have been determined [14-18], and one cytochrome c_7 from *Desulfuromonas acetoxidans* (*Da*) was structurally characterized by both nuclear magnetic resonance [19, 20] and X-ray crystallography [21]. A number of cytochromes c_7 are found in the genomes of δ-proteobacteria bacteria (e.g., five in *Gs* [the topic of this paper], five in *Geobacter metallireducens*, four in *Geobacter uraniireducens*, four in *Aneromyxobacter dehalogenans*, and three in *Da*). Interestingly, to the best of our knowledge, only the δ-proteobacteria encode either the cytochrome c_7 or cytochrome c_3 family. The only exception we found was one cytochrome c_3 homolog (SSed_2708; gi

* Corresponding author. Tel.: +1 630 252 3883; fax: +1 630 252 3387.
E-mail address: mschiffer@anl.gov (M. Schiffer).
[1] Present address: Y.Y. Londer, New England Biolabs, 240 County Road, Ipswich, MA 01938, USA.

0005-2728/$ – see front matter © 2009 Elsevier B.V. All rights reserved.
doi:10.1016/j.bbabio.2009.10.007

157375843) from *Shewanella sediminis* belonging to γ-proteobacteria. This gene is encoded within a genomic region (Ssed_2704 through Ssed_2732) in which most genes are unique to *S. sediminis*, suggesting that the entire locus might have origins outside the *Shewanella* genus (Dr. Margaret F. Romine, Pacific Northwest National Laboratory, Richland, WA, personal communication).

We are studying the triheme cytochromes c_7 family, members of which play an important role in the reduction of Fe(III) by *Gs* [22–24]. In their characterization of the periplasmic triheme cytochrome c_7 from *Gs* (GSU0612), PpcA (periplasmic cytochrome A), Lloyd et al. [22] showed that isolated PpcA can reduce Fe(III) and U(VI) *in vitro*. We previously expressed PpcA in *Escherichia coli* [25] and determined its three-dimensional structure at 1.45 Å resolution [26]. Further, we identified several sequences homologous to PpcA in the *Gs* genome [26]. Four of these are of the same size as PpcA: PpcB (GSU0364), PpcC (GSU0365), PpcD (GSU1024), and PpcE (GSU1760). Three other proteins identified as homologous to PpcA were large multiheme cytochromes that we previously reported as being composed of c_7-type triheme domains [26–29]. We have also described the microscopic reduction potentials of the individual hemes of PpcA [30] and the crystal structure of PpcB and partial characterization of PpcB heme redox properties [31]. The detailed thermodynamic characterization of the redox centers of PpcA, PpcB, PpcD, and PpcE will be described elsewhere (Dr. C.A. Salgueiro, private communication).

In the present paper, we report the crystal structures of PpcC, PpcD, and PpcE. To our knowledge, this is the first time that an entire family of cytochromes from one organism has been structurally characterized and compared with each other. These structures together with functional studies will aid in understanding the physiological roles of this family of cytochromes in microbial dissimilatory Fe(III) respiration.

2. Materials and methods

The procedures for isolation, crystallization, and structure determination employed for the three cytochromes c_7 homologs (PpcC, PpcD, and PpcE) are described here. Though the procedures for PpcA and PpcB were previously reported [26,31], their crystallization conditions are relevant to the present discussion and are included.

2.1. Bacterial strains and plasmids

E. coli strains DH5α (Invitrogen) and JCB7123 (BL21 [DE3] for PpcC) were used for cloning and expression, respectively [29,32]. Cultures were grown in 2× YT medium or on 2× YT agar plates [33]. Growth media were supplemented with carbenicillin (100 μg/mL) and, where appropriate, chloramphenicol (34 μg/mL). Plasmid pEC86, a derivative of pACYC184, containing the *ccm* gene cluster [34] was a kind gift from Dr. L. Thöny-Meyer (ETH, Zürich, Switzerland).

2.2. Cloning, expression, and purification of PpcC, PpcD, and PpcE

The DNA fragments coding for mature sequences were amplified from *Gs* genomic DNA, digested with restriction enzymes *Not*I and *Hin*dIII (*Not*I and *Eco*RI for PpcC) and cloned into vector pVA203 [27]. The vector was digested with the same enzymes. In all cases, the expression strains were co-transformed with plasmid pEC86 [34]. The proteins were produced in *E. coli* strain JCB7123, except PpcC which was produced in *E. coli* strain BL21 (DE3). The expression protocol was the same as for PpcA [25], with the exception that 10 μM IPTG was used for induction of PpcC and PpcD, while 200 μM IPTG was used for PpcE. The protein was purified by cation exchange and gel filtration column chromatography according to the approach used for PpcA [25,26]. The final yields of purified protein per liter of culture were 2 mg/L (PpcC and PpcD) and 3 mg/L (PpcE).

2.3. Crystallization

Purified and concentrated proteins (phosphate buffer pH 7.8, 0.1 M NaCl) were used to search for crystallization conditions by the hanging-drop vapor diffusion method and Hampton Research (www.hamptonresearch.com) screening kits: SaltRx, Index, Crystal Screen, and PEG/Ion. Protein (1 μL) was mixed with crystallization screening solution (1 μL) and equilibrated against a reservoir of 0.5 mL containing the screening solution. The crystals used for data collection were obtained under the following conditions: (a) For PpcC (protein at 17 mg/mL), structure was determined from a crystal obtained from SaltRx-70 (1.5 M lithium sulfate monohydrate, 0.1 M sodium acetate pH 4.6) and refined with data collected on a crystal obtained from a 4:1 dilution of SaltRx-64 with water (2 M ammonium sulfate, 0.08 M sodium acetate pH 4.6). (b) For PpcD (protein at 40 mg/mL), crystal was grown from Index-95 (30% w/v polyethylene glycol monomethyl ether 2000, 0.1 M potassium thiocyanate). (c) For PpcE (protein at 25 mg/mL), microcrystals obtained from SaltRx-31 (3.5 M sodium formate, 0.1 M bis–Tris propane pH 7.0) were optimized by the microseeding method. (d) For PpcA (protein at 24 mg/mL), crystals were grown from 3.5 M ammonium sulfate (pH adjusted to 6.0 with ammonium hydroxide), 0.25% deoxycholic acid [26]. (e) For PpcB (protein at 25 mg/mL), crystal was obtained from 45% Jeffamine ED-2001, 0.2 M ammonium iodide [31].

2.4. Data collection and structure determination

The cryoprotection solutions used for data collection were as follows: PpcC, 30% sucrose dissolved in SaltRx-64; PpcE, 26% sucrose in SaltRx-31; PpcD, reservoir solution used without modification. The crystals were transferred to the cryoprotecting solution for 15–30 s prior to freezing by direct placement in liquid nitrogen. The structures of PpcD and PpcE were determined by the multiple-wavelength anomalous dispersion (MAD) method by using data sets collected at three and four wavelengths, respectively, with data collected at the Fe K-edge at the Structural Biology Center's beamline 19BM, at the Advanced Photon Source (APS) at Argonne National Laboratory, Illinois. The structure of PpcC was

Table 1
Crystal and refinement parameters for the c_7 homologs.

	PpcB	PpcC	PpcD	PpcE
Crystal parameters				
a (Å)	34.2	79.2	27.4	37.7
b (Å)	47.5	79.2	55.9	102.0
c (Å)	88.9	67.1	94.8	22.7
Space group	$P2_12_12_1$	$P4_12_12$	$P2_12_12_1$	$P2_12_12$
No. molecules/AU	2	1	2	1
V_M[a]	1.89 (34.8)	5.28 (76.7)	1.90 (35.2)	2.26 (45.5)
Refinement				
Program used	Refmac5	Refmac5	Refmac5	CNS
Resolution range (Å)	19.5–1.35	15–2.25	36–1.35	30–1.6
σ cutoff used	0.0	0.0	0.0	0.0
No. reflections	27,324	8,938	28,548	10,806
R-factor	0.161	0.203	0.149	0.190
R-free	0.185	0.241	0.172	0.205
No. non-hydrogen atoms (average *B*-factor, Å^2)[b]				
Protein	534 (8.7) 534 (7.7)	542 (37.2)	498 (8.8) 507 (10.7)	546 (12.2)
Heme	129 (6.2) 129 (6.9)	129 (28.2)	129 (6.3) 129 (8.0)	129 (10.4)
Water	108 (24.0) 98 (24.1)	44 (46.4)	104 (21.7) 91 (23.7)	103 (22.7)
PDB entry	3BXU	3H33	3H4N	3H34

[a] Percent estimated solvent content is shown in parentheses.
[b] For PpcB and PpcD structures, average of the equivalent isotropic *B*-factor is shown for the protein and heme atoms.

Table 2
Properties of the c_7 homologs.

	PpcA	PpcB	PpcC	PpcD	PpcE
No. residues	71	71	75	72	70
Calculated pI[a]	9.2	9.0	8.8	9.0	9.5
% CD signal at 90 °C compared to 25 °C[b]	81	72	74	69	36
Instability index[c]	33	38	37	46	53

[a] pI values calculated by ProtParam (http://ca.expasy.org/tools/protparam.html) using amino acid sequence only not including the heme propionic acids.
[b] Stability, measured as change in circular dichroism with temperature at the heme absorption (Soret) band.
[c] Instability index calculated by ProtParam (http://ca.expasy.org/tools/protparam.html).

determined by the single-wavelength anomalous dispersion (SAD) method, with the X-ray diffraction data collected at room temperature by using the laboratory rotating-anode generator (RU200, Rigaku; Ni-filtered Cu K_α radiation, $\lambda = 1.54$ Å) and an R-Axis IIc imaging plate detector (Rigaku). Details of the MAD and SAD data sets used for structure determination are in Table S1 of the Supplementary data. Data used for refinement in each case were collected at 100 K and 12 keV at 19BM (APS). Diffraction data were processed by using HKL2000 [35]. The structures were solved with the program CNS [36]. The electron density maps calculated with CNS after the density modification procedure were of excellent quality; models were built manually into the maps by using the program Chain [37] and refined against the high-resolution data with the program CNS or Refmac [38]. In the final stage of refinement, all non-hydrogen protein atoms of PpcB and PpcD structures were refined with anisotropic displacement parameters. The crystal and refinement parameters are summarized in Table 1.

2.5. Stability determination

Circular dichroism (CD) spectra were collected on a Jasco J-810 spectropolarimeter. Spectra in the wavelength ranges 190–260 nm (far ultraviolet [UV] region) and 350–450 (heme absorption region) were obtained (0.1-nm steps, 1-nm bandwidth, 4-s response, 100-millidegree sensitivity, 50 nm/min scanning speed with accumulation 3) in a 0.1-cm-pathlength quartz cell. For estimation of thermal stability, spectra in both the UV and visible regions were measured as a function of temperature from 20 °C to 90 °C in 5-deg intervals as described by Dolla et al. [39].

2.6. Determination of heme puckering

The distortion of the heme porphyrin rings was determined by the Normal-Coordinate Structural Decomposition method (http://jasheln.unm.edu/jasheln/content/nsd/NSDengine/start.htm) and plotted as previously reported [40].

3. Results and discussion

3.1. Properties of the cytochromes c_7 homologs from Gs

The properties of the homologs are summarized in Table 2. Theoretical pI values (estimated based on protein sequence excluding the heme carboxylic acid groups) by using ExPASy-ProtParm tool (http://ca.expasy.org/tools/protparam.html) of approximately 9 for all homologs indicate that these proteins are very basic; PpcE is the most basic (pI = 9.5), followed by PpcA (pI = 9.2). The homologs are very stable (Table 2), as expected from covalent linkage of three hemes to the polypeptide chain and the bis–His axial ligation of each heme. PpcE had the lowest stability, with a T_m value of 85 °C. We could not estimate T_m for the other homologs from the temperature dependence of CD curves, as these homologs were stable in the temperature range studied [data not shown]). This result correlates well with the observation that PpcE has the highest instability index among the homologs (Table 2), as calculated (based only on amino acid sequence and not including the heme cofactors) by using the ExPASy-ProtParm tool (http://ca.expasy.org/tools/protparam.html).

3.2. Overall description of the cytochromes c_7

The cytochromes c_7 are small proteins of approximately 70 amino acids, with three hemes bound to the protein through covalent bonds with the Cys residues in the heme-binding motif, CXXCH. The His residue in the heme-binding motif forms the fifth axial ligand to the heme, and another His residue located elsewhere in sequence forms the sixth axial ligand. To maintain consistency with the literature on structurally related cytochromes c_3, we number the heme groups in the triheme cytochromes c_7 as I, III, and IV. In the cytochromes c_7 and c_3 families, all the heme groups have bis–His axial coordination. The bis–His axial ligation and the fact that the hemes are well exposed to solvent in these proteins results in low heme reduction potentials (see reduction potential values for PpcA [30] and PpcB [31]). Therefore, cytochromes c_7 from *Gs* described here are expected

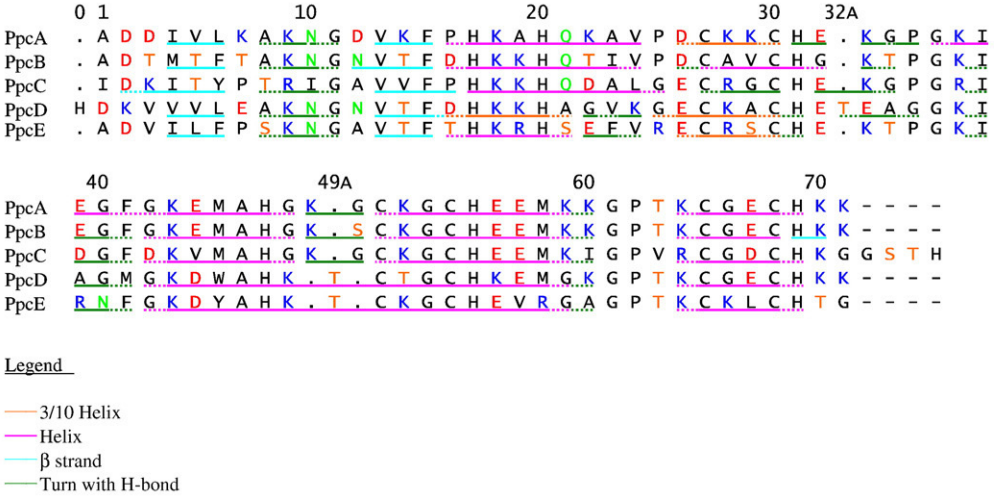

Fig. 1. Structure-based sequence alignment of cytochromes c_7 from *Gs*. Aligned sequences of the homologs illustrate the different distributions of charged and polar residues (acidic residues Asp and Glu in red; basic residues Lys and Arg in blue; polar residues Asn and Gln in green; and Ser and Thr in orange). Insertions and deletions of residues result in different spatial arrangements of side chains and cause variations in surface electrostatic potential.

Table 3
Percentage sequence identities (calculated from the structure-based sequence alignment shown in Fig. 1) of the cytochromes c_7 from *Geobacter sulfurreducens*.

	Identity (%)			
	PpcB	PpcC	PpcD	PpcE
PpcA	77	63	60	56
PpcB		58	58	58
PpcC			45	52
PpcD				53

to be fully oxidized under the conditions used for their isolation and crystallization.

The cytochromes c_7 structures are composed of conserved secondary structural features comprising a two-strand β-sheet at the N-terminus, followed by several helical regions. The helical segments contain Cys residues linked to heme cofactors and also axial His ligands. The cytochromes c_7 family members PpcB, PpcC, PpcD, and PpcE have very similar heme core structures. Their overall protein folds are the same, but some local structural differences are present. Even though the secondary-structure elements are conserved between different proteins, they do not necessarily overlap with each other when the whole molecules are overlapped (see Section 3.3). PpcA is included only in sequence comparisons in this paper; it is not used for structural comparisons, because its structure as observed in the crystal was different from that of the other homologs; the additive deoxycholate used in crystallization was bound to PpcA and altered its structure in the crystal (see Sections 3.8 and 3.9 for further discussion).

3.3. Sequence and structural comparison

Fig. 1 shows the structure-based amino acid sequence alignment of the five cytochromes c_7, together with their corresponding secondary structures. The percent sequence identities between the five c_7 homologs are shown in Table 3. The alignment of the sequences (Fig. 1) shows that in the middle of the protein chain, PpcD has an insertion, Thr (32A), after the heme I binding motif. The structure of the chain segment from residues 16 to 41, except for the residues in the heme I binding motif, is different in PpcD than in the other homologs. PpcD and PpcE have one fewer residue before the heme III binding motif. Although the Lys before the heme III binding sequence (at position 49 in PpcA; see Fig. 1) appears to be conserved in sequence in all five proteins, it is structurally equivalent to the same residue in only PpcB and PpcC. Therefore, on the basis of structural comparisons, this Lys in PpcD and PpcE is

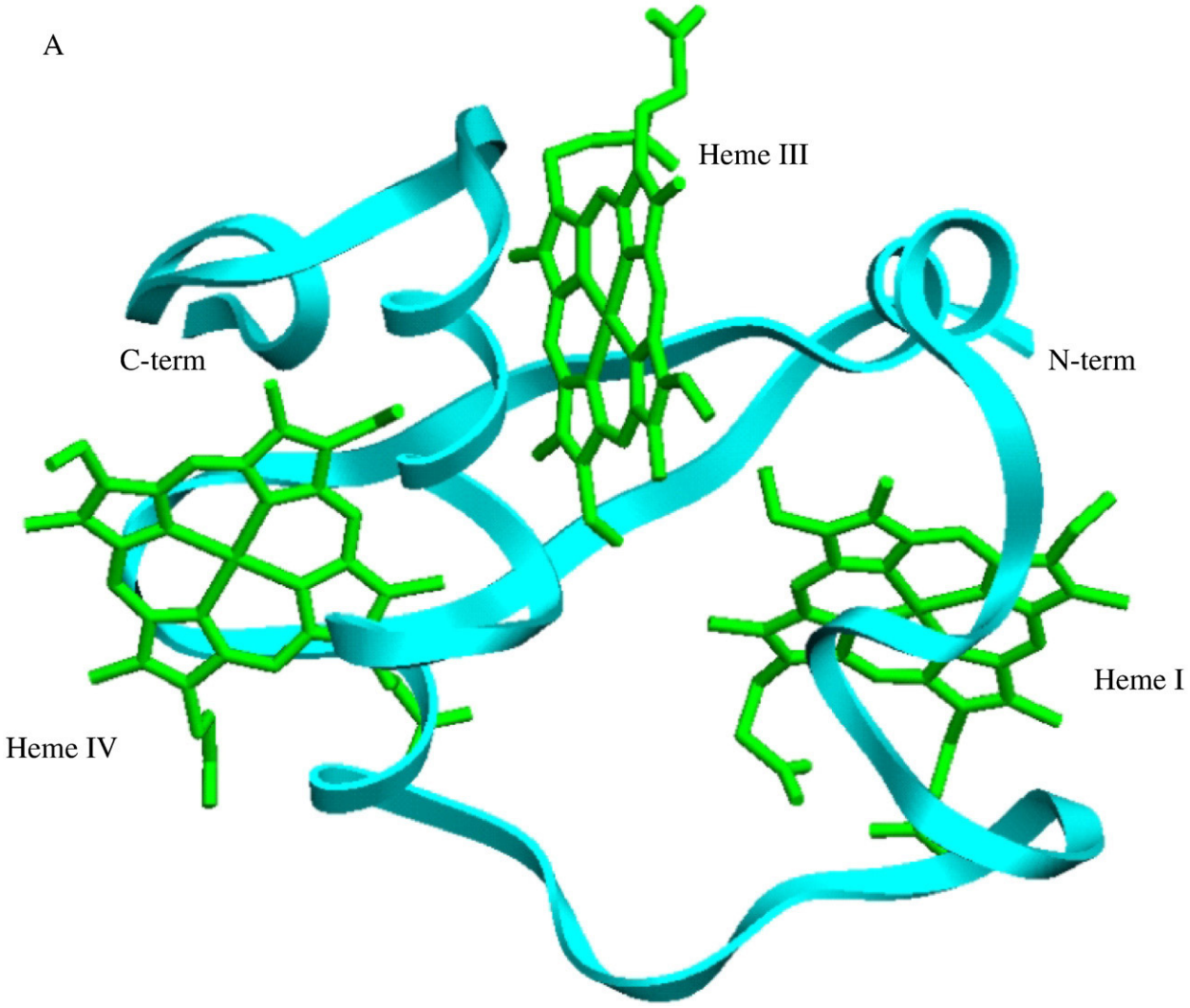

Fig. 2. (A) Structure of cytochrome c_7 PpcB. Hemes are shown in green, and the polypeptide is shown as a blue ribbon. (B) A stereo view of the heme core arrangement. PpcC (blue), PpcD (gray), and PpcE (red) were overlapped on PpcB (green) by using all three heme ring atoms, including Fe. (C) A stereo view of the overlap of C_α atoms of PpcB (green), PpcC (blue), PpcD (gray), and PpcE (red). The residue labels correspond to PpcB, except for 32A and 49A from PpcD. (D). A stereo view of the overlap of PpcB (black) and PpcD (gray). Note the deviations in the polypeptide chain between residues 16 and 41, except for the heme-binding residues 27–31.

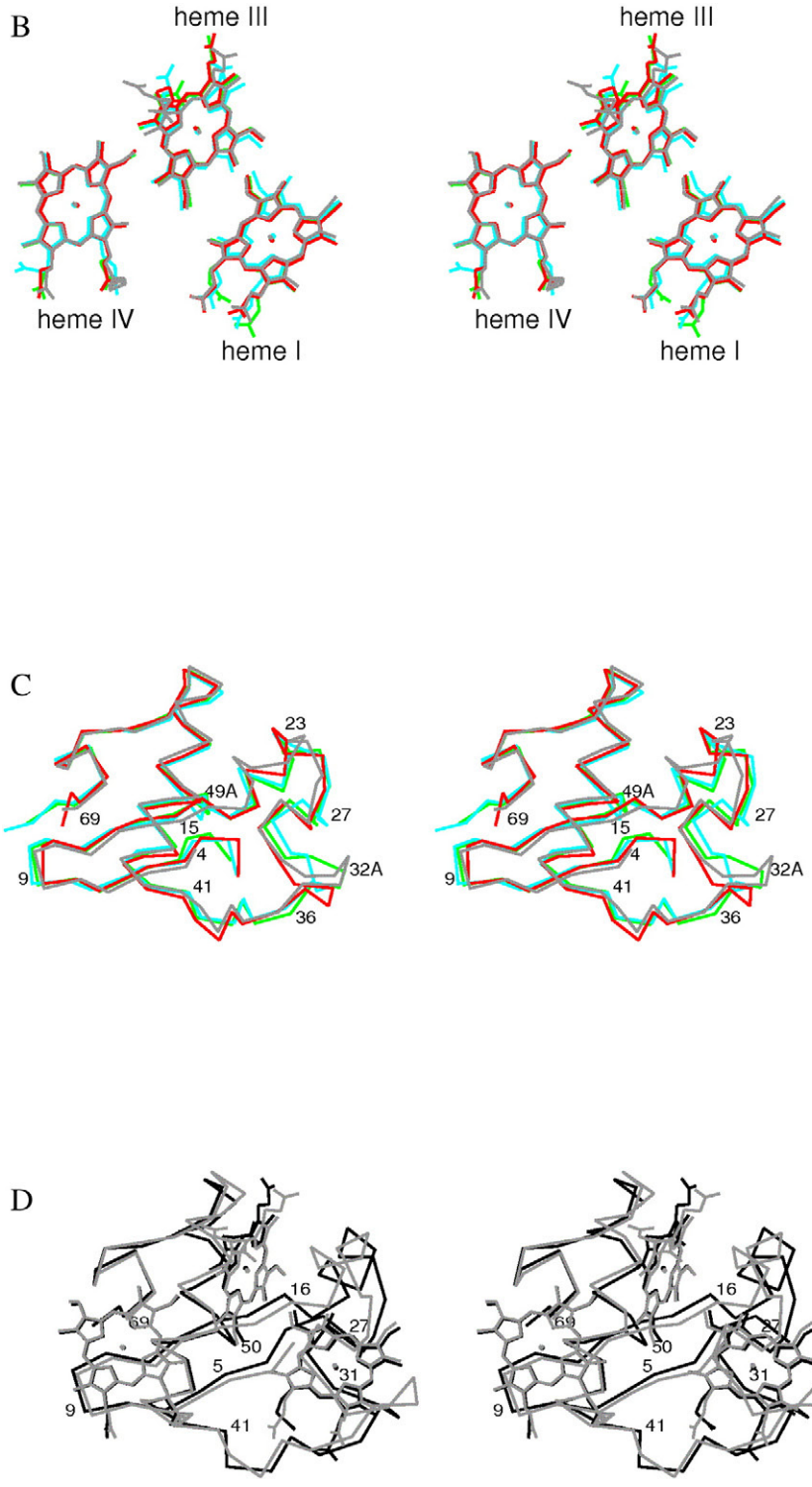

Fig. 2 (*continued*).

equivalent to Gly48 in PpcA (as well as in PpcB and PpcC), and the Thr present after this Lys in the sequences of PpcD and PpcE at this location is not equivalent to any of the residues in the other three proteins. Consequently, we labeled this residue as Thr49A in the sequence alignment. With one fewer residue at this site, PpcD and PpcE form regular helices, whereas PpcA, PpcB, and PpcC have a bulge in the alpha helix at this position.

The typical cytochrome c_7 structure observed for these molecules is illustrated by protein PpcB in Fig. 2A. The structures of homologs were compared by overlapping different sets of atoms from each structure by using the program Profit (Martin, A.C.R. and Porter, C.T. http://www.bioinf.org.uk/software/profit/). The overlaps between different protein structures were accomplished with the following atoms: method A, all three heme porphyrin ring atoms including Fe atoms (heme core); method B, alpha carbons of residues 5–69; and method C, alpha carbon atoms of residues 5–15 and 41–69 (residues around heme IV). The residues in insertions and deletions (such as residues 32A, 49, 49A, and 50) were not included in the calculations.

Table 4
Root mean square deviation values of the homologs overlapped by three different methods.[a]

	RMSD (Å) for methods A, B, and C				
	PpcB_B	PpcC	PpcD_A	PpcD_B	PpcE
PpcB_A	0.3; 0.6; 0.3	0.4; 0.9; 0.4	0.3; 1.8; 0.5	0.3; 1.7; 0.4	0.2; 0.9; 0.5
PpcB_B		0.3; 0.7; 0.3	0.4; 2.0; 0.5	0.5; 1.9; 0.5	0.4; 1.0; 0.5
PpcC			0.5; 2.2; 0.7	0.5; 2.1; 0.6	0.5; 1.2; 0.6
PpcD_A				0.1; 0.4; 0.3	0.4; 1.7; 0.6
PpcD_B					0.4; 1.6; 0.5

[a] The RMSD values were generated with the program Profit by using overlap methods A, B, and C. Atoms used for overlap are (method A) all three heme porphyrin ring atoms, including Fe atoms; (method B) alpha carbons of residues 5–69; (method C) alpha carbon atoms of residues 5–15 and 41–69. In methods B and C, the insertions and deletions for each protein were excluded. PpcB and PpcD have two independent molecules in the crystals, represented by A and B.

The root mean square deviations (RMSD values) are in Table 4. A stereo view of the overlapped hemes (method A above) for the homologs is shown in Fig. 2B, and the corresponding C_α tracing is in Fig. 2C. The heme core arrangement is generally maintained between the homologs, while the polypeptide chain surrounding the hemes tends to have variations between proteins (see Fig. 2B and C; compare RMSD values A and B in Table 4). Higher deviations in the structures were generally found in the residue range 16–40 (see Fig. 2C) that is evident when the RMSD values were compared between overlaps B and C (Table 4). The structural similarity between the proteins is highest near heme IV and lowest near heme I (Fig. 2). The overlaps also demonstrate that PpcD is the most different from the other cytochromes c_7 (see Table 4 and Fig. 2D).

3.4. Conserved residues

In the five homologs, 23 residues are identical. Of these, 12 are heme-binding residues (2 Cys and 2 His residues for each heme); the other 11 conserved residues are Gly11, Gly36, Gly53, and Gly61; hydrophobic residues Val13, Phe15, Ile38, and Ala46; Pro62; Lys18; and Lys43 (Fig. 1). All conserved glycines (except for 53) in this family have phi and psi angles that would not allow side chains at these positions. The Gly11 carbonyl forms a hydrogen bond with His69, and Gly36 forms a hydrogen bond with His31; Gly61 is close to heme III and has unusual phi and psi angles; Gly53 is in an alpha helix as part of the heme III binding motif on the surface of the protein, with no obvious reason for its conservation. The conserved hydrophobic residues are close to the hemes: Val13 is close to heme III; Phe15 is between hemes I and III; Ile38 is close to heme I and protects heme I and His 31 from exposure to the solvent, and its peptide nitrogen forms a hydrogen bond with the propionic acid of heme I; Ala46 is located between Phe41 and heme IV, where there is no room for any residue with a larger side chain; Pro62 is close to heme III and is almost parallel to the ring of His 55; and Pro62 also forms a hydrogen bond with the side chain of His55. Residue Lys43 is conserved because it forms van der Waals interactions with heme IV. There is no obvious reason for the conservation of Lys18, which is on the surface. Conservation of many of the above residues in cytochromes c_7 from other organisms (Fig. S1 of the Supplementary data) shows that they have an important role in the three-dimensional structures of the cytochromes c_7. No conserved hydrogen bonds occur between side chains.

Table 5
Heme geometry and solvent exposures.

	PpcC	PpcD[a]	PpcE	PpcB[a]	*Da* c_7[b]	PpcA
Heme Fe–Fe distance (Å)						
I–III	11.2	11.2 (11.3)	11.8	11.7 (11.5)	11.5	11.2
I–IV	18.5	18.2 (18.2)	18.2	18.2 (18.8)	19.3	20.8
III–IV	12.6	12.6 (12.6)	12.4	12.6 (12.8)	12.6	12.6
Angle between heme planes (°)						
I–III	81	78 (76)	71	73 (72)	81	86
I–IV	18	25 (24)	22	20 (16)	8	35
III–IV	75	72 (70)	72	70 (71)	77	69
Angle between axial His ring planes (°)						
Heme I: His17–His31	52	12 (3)	77	79 (88)	79	57
Heme III: His20–His55	38	38 (22)	34	35 (36)	31	22
Heme IV: His47–His69	86	85 (84)	89	75 (81)	83	89
Heme solvent exposure ($Å^2$)						
I	213	210 (219)	215	188 (210)	223	225
III	166	160 (187)	129	156 (145)	210	144
IV	188	188 (184)	189	187 (189)	242	189

The crystal structure of PpcA differs from the other c_7s but the relevant data are included only for the sake of completeness and not for comparison (see Results and discussion section).

[a] The values in parentheses for PpcD and PpcB are corresponding values for monomer B.

[b] The values are taken from Ref. [21], except for the heme solvent exposures calculated by us.

3.5. Description of the heme cores

The heme core arrangement of the cytochromes c_7 is well conserved, as evidenced by the distances between the iron atoms of the hemes and the angles that the heme porphyrin ring planes make with each other within the molecules (Table 5), except for PpcA, as mentioned previously. (PpcA is included in Table 5 only for the sake of completeness.) Heme I and heme IV are almost parallel with each other, while they are both nearly perpendicular to heme III. Heme III is in van der Waals contact with both hemes I and IV. The axial His geometry is fairly conserved in all cases, except for heme I in PpcD. The angle between the coordinating His ring planes differs most for heme I of PpcD, where the two His rings are nearly parallel with each other; in the other homologs, the same angle is closer to perpendicular. This difference results from the variation of structure in PpcD involving residues 16–41, which placed the backbone of His17 in a different location, though its coordinating nitrogen atom of the histidine ring is in the same place as that in the other homologs (see Section 3.3 and Fig. 2D). The two molecules in the crystal of PpcD have close to the same structure suggesting that this difference between PpcD and other homologs is not a result of crystal packing. The difference in heme I axial His ring orientations was further confirmed by the analysis of the NMR heme methyl chemical shifts (Dr. C.A. Salgueiro, private communication). A conserved feature of all cytochromes is a hydrogen bond between the axial His $N\delta_1$ atom and a peptide oxygen or a water molecule. This feature is maintained in this family of cytochromes c_7 from *Gs*. Comparison revealed that heme I generally has the highest solvent exposure, while heme III has the lowest; the solvent exposure of heme III is especially low in PpcE (Table 5).

The cytochrome c_7 from *Da* is the only other triheme cytochrome for which a crystal structure is available [21]. Its sequence identity with the *Gs* cytochromes c_7 is in the range of 44–56%. The heme core arrangement in *Da* cytochrome c_7 differs from that in the family of *Gs* cytochromes c_7. This is evident in the heme Fe–Fe distance of 19.3 Å between hemes I and IV in *Da* cytochrome c_7 (taken from PDB entry, 1HH5), compared to an average of 18.3 Å in *Gs* cytochromes c_7 (this study; Table 5). The Fe–Fe distances between hemes I and III (11.5 Å) and hemes III and IV (12.6 Å) in *Da* cytochrome c_7 are quite similar to the corresponding values in *Gs* cytochromes c_7 (see Table 5). These variations in the structures of cytochromes c_7 underscore the structural flexibility of these molecules (see Section 3.8 for more discussion on the flexibility).

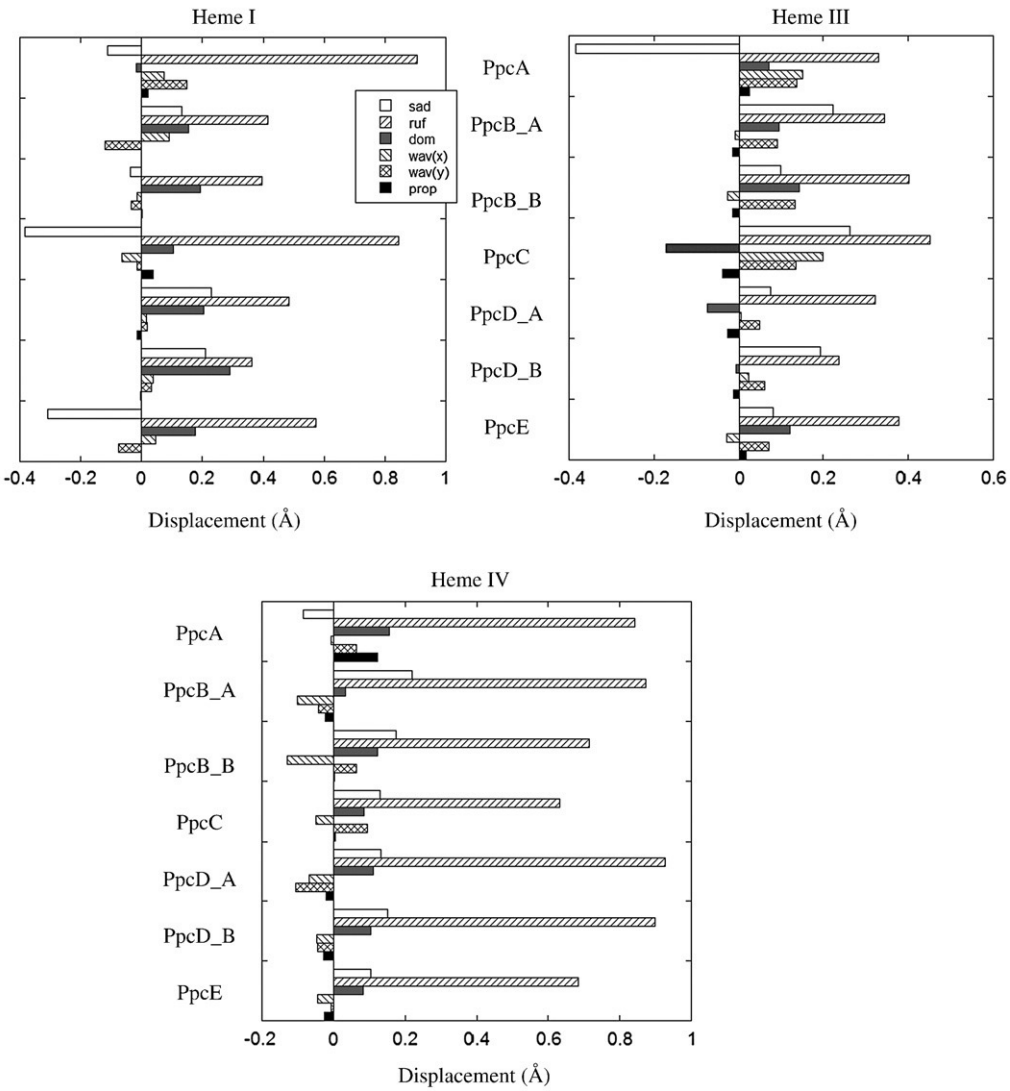

Fig. 3. Heme porphyrin distortions in the family of cytochromes c_7 from *Gs*. The six displacement parameters for each of the hemes from all proteins (Å, horizontal axis) were calculated by the normal-coordinate structural decomposition method [40]. PpcC structure was determined at a relatively lower resolution (2.25 Å) and hence there is less confidence in these values.

Interestingly, the heme core arrangement is somewhat less compact in cytochromes c_7 than in cytochromes c_3, as is evident in the Fe–Fe distances between the hemes. The largest deviation occurs between hemes I and IV (average values, 18.4 Å in c_7 versus 17.7 Å in c_3), followed by hemes III and IV (average values, 12.6 Å in c_7 compared with 12.1 Å in c_3), and then hemes I and III (average values, 11.5 Å in c_7 compared with 11.1 Å in c_3). The average Fe–Fe distances for cytochromes c_7 are calculated from structures of the cytochrome c_7 family from *Gs*, and those of cytochromes c_3 are taken from Table 3 of reference 26. The reasons for the above differences in heme core arrangements between the two related families of proteins are not clear.

3.6. Conformation of the heme planes

The porphyrin ring distortions reflect the forces exerted by the protein environment on each heme. Thus, it is of interest to compare the heme puckering in the family of cytochromes c_7 from *Gs* with highly homologous sequences and structures. Fig. 3 shows the distortion of the hemes as calculated by the normal-coordinate structural decomposition method [40]. Previously, heme puckering was related to the number of residues between the Cys residues binding the hemes in the cytochrome c_3 family, where hemes I and III are bound to CX_2CH motifs and hemes II and IV are bound to CX_4CH motifs [40]. In several structures of cytochromes c_3, hemes II and IV are clearly more puckered than hemes I and III [40]. This explanation clearly cannot account for the observed variations in the porphyrin distortions in the cytochrome c_7 family, as there are only two residues between the Cys residues binding each heme, and the two residues are conserved for some of the proteins (see Fig. 1). It is more likely that differences between proteins in the residues forming the pocket for each heme contribute to the variation in porphyrin ring distortions. Heme IV, the most puckered, has similar structure in all of the homologs. Hemes I and III are more flat than heme IV (Fig. 3). The confidence in heme puckering values is lower in the PpcC structure because it was determined at a lower resolution (2.25 Å) compared to other homologs.

3.7. Hydrogen bonds to the hemes

In all homologs, the heme groups are arranged such that their propionic acid groups are facing the surface of the protein. The following hydrogen bonds or salt bridges with the propionic acids of the hemes are conserved in the different homologs. The peptide

nitrogen of conserved residue Ile38 forms a hydrogen bond with propionic acid of heme I. A salt bridge is present between Lys37 (Arg in PpcC) and propionic acid of heme I. A salt bridge is formed by Lys19 (Arg in PpcE) with the propionic acids of heme III. The peptide nitrogen of residue Lys9 (Arg in PpcC) forms a hydrogen bond with the propionic acid moiety of heme IV.

Additional non-conserved hydrogen bonds and salt bridges that might influence the heme properties of individual proteins are as

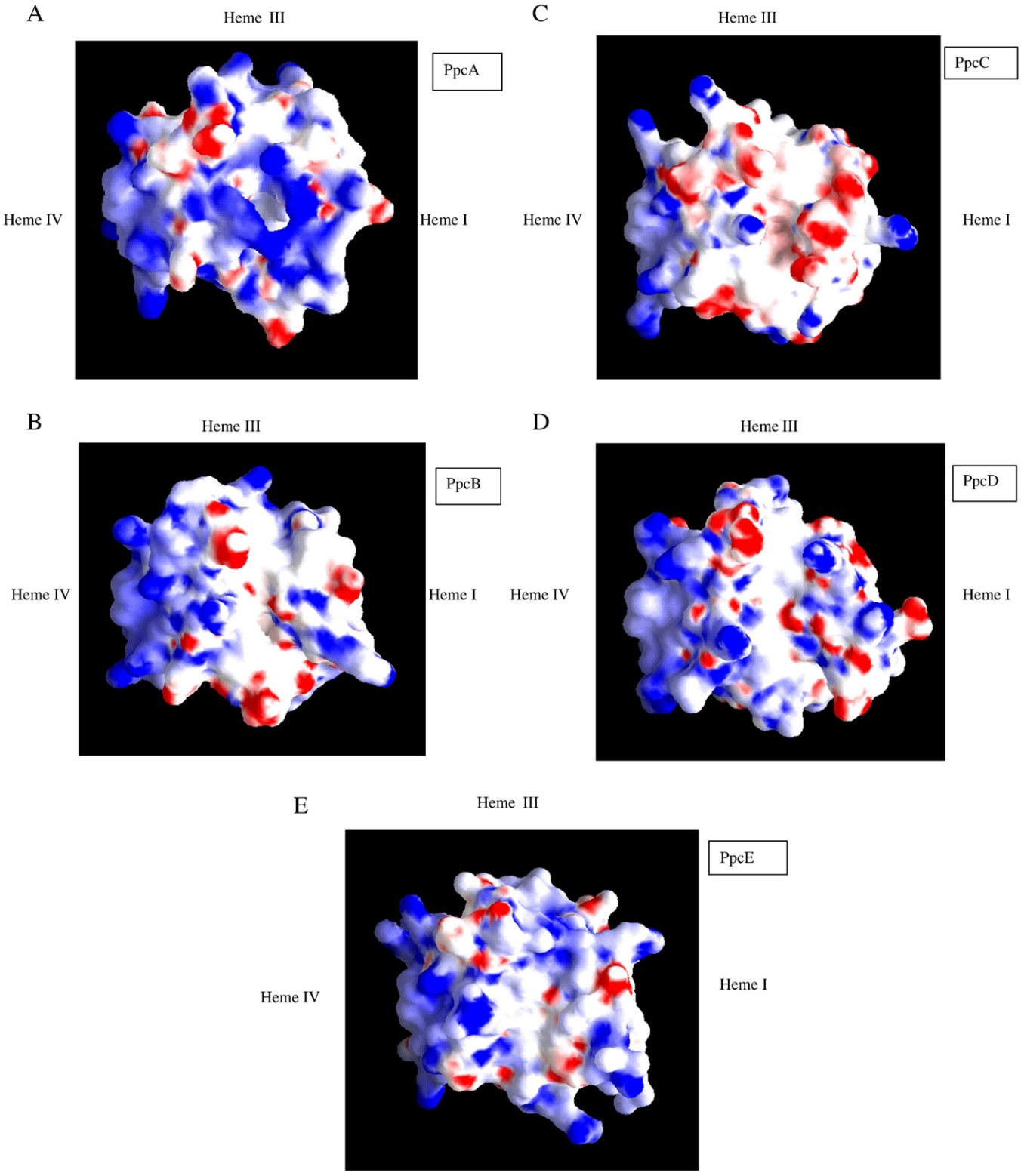

Fig. 4. Electrostatic potential on the surface of the cytochromes c_7 (negative potential in red; positive potential in blue). PpcA, PpcB, PpcC, PpcD, and PpcE are shown in A, B, C, D, and E respectively. The molecules are in the same relative orientation and approximately in the orientation of the molecule shown in Fig. 2A, with heme I on the viewer's right, heme III at the top, and heme IV on the left. PpcC, PpcD, and PpcE were overlapped on PpcB by using all three heme porphyrin ring atoms; PpcA was overlapped on PpcB by using heme III and heme IV porphyrin ring atoms only. In the case of PpcA (A), an excess positive charge surrounds a cavity in the middle of the figure that is the binding location of the anionic molecule deoxycholate. The absence of such a feature in the other homologs could explain why the others do not require deoxycholate for crystallization.

follows: In PpcC, the hydroxyl group of Tyr6 is 3.9 Å from propionic acid of heme I; none of the other homologs have a polar group at position 6. An additional hydrogen bond is observed in PpcC between the peptide nitrogen of Ile10 and the heme IV propionic acid. Lys60 (present only in PpcB and PpcD) is within a distance that could form a salt bridge with the heme III propionic acid. In PpcE, Thr16 forms a weak hydrogen bond (3.4 Å) with the heme III propionic acid.

3.8. Flexibility of structures

The structure of PpcA [26], the cytochrome c_7 found to be the most abundant in the periplasm of *Gs* [22], differs significantly from the structures of the other homologs. PpcA, as observed in its crystal structure, has a pocket where a guest molecule (deoxycholate) is bound; this feature is not observed in the structures of the other homologs. Deoxycholate was required for crystallization of PpcA (see also Section 3.9) but not of the other homologs. In PpcA, heme I and heme IV are farther apart, with a Fe–Fe distance of 20.8 Å, compared with an average of 18.3 Å in the other four structures (Table 5). Subsequently, we found that the heme core of PpcA in solution was very similar to that of PpcB [31]. This unexpected change in the relative arrangement of the hemes of PpcA in the crystal versus solution suggests that the heme core arrangement of the molecule is flexible. Also of interest is the differences between the two molecules in the unit cell of PpcB (PDB code, 3BXU), as illustrated best by the difference in the Fe–Fe distance between hemes I and IV of PpcB: 18.2 Å for monomer A and 18.8 Å for monomer B (Table 5). This difference in distance (0.6 Å) is larger than the error (~0.1 Å) in the Fe coordinates; the relative angles of the coordinating axial His rings to hemes I and IV of PpcB are also different between the two monomers (Table 5). This observation suggests that even the lattice forces that are different for the two molecules in the unit cell of the crystal can alter the structures of cytochromes c_7 to some extent.

3.9. Crystal packing

As expected from the variations in their sequences, all homologs crystallized under different conditions and in different packing arrangements. PpcB and PpcD formed very tightly packed crystals, both having a solvent fraction of 35% (see Table 1), whereas the solvent fraction for PpcE (45%) was in the normal range for protein crystals. PpcC formed loosely packed crystals (solvent fraction 77%). The examination of the crystal packing interactions in all five cytochrome c_7 homologs revealed that these molecules can employ heme–heme, protein–protein, and protein–heme interactions equally to exploit all possible crystal packing scenarios; no predominant packing pattern is observed in this family of crystal structures. Surprisingly, even though all of these cytochromes c_7 contain two conserved β-strands at the N-terminus, only in one case (PpcB, see below) is interaction observed between molecules in the crystal to form an extension of the β-sheet.

A remarkable packing interaction is observed in crystals of PpcD, which has two layers of molecules; within each layer, heme I of one molecule and heme IV of another molecule form edge-to-edge stacking interactions with heme planes almost parallel (see Fig. S2 of Supplementary data). This brings the hemes closer to each other (Fe–Fe distance = 9.9 Å) than any of the heme pairs within a molecule (the closest intramolecular Fe–Fe distance is >11 Å). This type of interaction, where hemes can be closer between different molecules than within a given molecule, may have implications for electron transfer between heme proteins.

Protein interface analysis of the crystal structures as routinely done in the PDB deposits by using the program PISA (www.ebi.ac.uk/msd-srv/prot_int/pistart.html [41]) suggested the presence of quaternary structure (dimers) in the crystals of PpcA, PpcB, and PpcC but not in crystals of PpcD and PpcE. The indications of dimerization observed in the molecular interface analysis of the crystals may be accidental to achieve optimum crystal packing. At 5 mg/mL, neither size-exclusion column chromatography nor dynamic light scattering studies (data not shown) yielded evidence in solution for dimerization of any of the homologs. NMR data also support the absence of any quaternary structure for these proteins in solution (Dr. C.A. Salgueiro, private communication). Thus, the dimers observed in crystals probably have no physiological relevance.

3.10. Conservation of structure and surface charge around heme IV

The structure of heme IV and its surroundings appear to be the most conserved among the cytochromes c_7 family studied, as can be seen in Table 5 and in Fig. 3. The solvent exposure (Table 5) and the puckering of heme IV (Fig. 3) in all the homologs are essentially the same. The distances between Fe atoms of hemes III and IV are most conserved in all homologs; they vary by less than 0.2 Å from the average. The RMSD values (Table 4, method C [overlap of alpha carbons close to heme IV]) also suggest similar protein structure in this region of the homologs, while the structures in the remainder of the molecules differ (method B). Although the variation in the distribution of charged residues resulted in different electrostatic potential values on the surfaces of these molecules, all of the cytochrome c_7 homologs had a positively charged surface near heme IV. Fig. 4 shows the electrostatic potential on the molecular surface of each cytochrome c_7, as calculated by the program GRASP [42].

3.11. Functional implications for the cytochrome c_7 family

At present, the exact functions of the cytochromes c_7 from *Gs* and *Da* are unknown. PpcA has the largest concentration in the periplasm and is one of the molecules in the electron transfer chain involved in acetate oxidation coupled to Fe(III) reduction by *Gs* [4, 22]. PpcB and PpcC are encoded on a contiguous gene fragment; this opens up the possibility that these two proteins are co-expressed and could interact with each other in the periplasm. Studies of mutant *Gs* strains carrying knockouts of the cytochromes c_7 displayed different iron reduction rates and different growth characteristics, implying a unique role for each of the proteins [11, 23, 24; Dr. Laurie DiDonato, University of Massachusetts, Amherst, unpublished results]. In knockout studies of the individual cytochromes c_7, the growth of mutant *Gs* strains on soluble or insoluble iron was affected. The work cited above indicated that the five homologs might be active in different iron reduction pathways in the periplasm and that they could also influence the expression of one another. Detailed biochemical studies of the knockout strains of *Gs* deficient in the cytochromes c_7 are required to shed more light on their individual functions.

All PpcA homologs have the lowest structural similarity near heme I and the highest near heme IV (see Fig. 2); in addition, all homologs have a positive electrostatic surface potential near heme IV (Fig. 4). These two observations (conserved structures and surface charge) together suggest that the homologs could interact with an identical or a similar physiological partner near heme IV. A large number of positively charged residues have been noted previously around heme IV in the case of cytochromes c_3 [43]. Based on NMR and docking experiments, the region around heme IV in cytochromes c_3 was proposed to be the site of interaction with their physiological partners [43–45]. The structures and surface charges of each of the cytochromes c_7 have prominent differences near heme I and heme III. Therefore, we postulate that each of these cytochromes could interact with different partners near heme I or heme III. This could account for the requirement for five similar proteins encoded by the genome of *Gs*.

Interestingly, PpcD is the only member of the c_7 family that was found to be more abundant in the cells of *Gs* grown with the insoluble

Fe(III) oxide as electron acceptor than with the soluble electron acceptor Fe(III) citrate [46]. Our structural results showing that PpcD is the most different among the c_7 homologs could suggest an important albeit unknown role for this protein in Fe(III) oxide reduction.

4. Conclusions

The work presented in this paper represents the structural characterization and comparison of an entire family of five similar electron transfer proteins from one organism, *G. sulfurreducens*. The sequence identity between the five cytochromes c_7 studied varies between 45% and 77%. The proteins have a very similar fold and their triheme core arrangements. We observed local differences in structure and surface characteristics. The heme IV region in all cytochromes c_7 is probably the site of interaction with the same or similar physiological partner. The other interacting partner, which may be different for each homolog, will interact near the heme I or heme III region. The similarities and differences in the structures and properties of the cytochromes c_7 family are very likely to play a role in the way the organism exploits the available range of redox partners and conditions to achieve versatility in respiratory mechanisms. The high-resolution structures presented here will make it possible to determine electron transfer pathway and its coupling to proton transfer in these molecules by computational methods and suggest which residue or a set of residues can influence the pathways.

Acknowledgments

The work at Argonne National Laboratory was supported by the U.S. Department of Energy's Office of Science, Biological and Environmental Research GTL program under contract No. DE-AC02-06CH11357. Use of the Structural Biology Center beamlines was supported by the U.S. Department of Energy's Office of Biological and Environmental Research. Use of the Advanced Photon Source was supported by the U. S. Department of Energy, Office of Science, Office of Basic Energy Sciences. Prof. C.A. Salgueiro (FCT/UNL, Lisbon) contributed many useful discussions and critical reading of the manuscript. This work is a part of collaboration with Prof. D. R. Lovley (University of Massachusetts, Amherst) under the Genomics:GTL project.

Appendix A. Supplementary data

Supplementary data associated with this article can be found, in the online version, at doi:10.1016/j.bbabio.2009.10.007.

References

[1] D.R. Lovley, Cleaning up with genomics: applying molecular biology to bioremediation, Nat. Rev., Microbiol. 1 (2003) 35–44.
[2] J.R. Lloyd, D.R. Lovley, Microbial detoxification of metals and radionuclides, Curr. Opin. Biotechnol. 12 (2001) 248–253.
[3] D.R. Lovley, Extracellular electron transfer: wires, capacitors, iron lungs, and more, Geobiol. 6 (2008) 225–231.
[4] D.R. Lovley, Bug juice: harvesting electricity with microorganisms, Nat. Rev. Microbiol. 4 (2006) 497–508.
[5] K.P. Nevin, H. Richter, S.F. Covalla, J.P. Johnson, T.L. Woodard, A.L. Orloff, H. Jia, M. Zhang, D.R. Lovley, Power output and columbic efficiencies from biofilms of *Geobacter sulfurreducens* comparable to mixed community microbial fuel cells, Environ. Microbiol. 10 (2008) 2505–2514.
[6] D.R. Lovley, K.P. Nevin, Electricity production with electricigens, in: J. Wall, et al., (Eds.), Bioenergy, ASM Press, Washington, DC, 2008, pp. 295–306.
[7] B.A Methé, K.E. Nelson, J.A. Eisen, I.T. Paulsen, W. Nelson, J.F. Heidelberg, D. Wu, M. Wu, N. Ward, M.J. Beanan, R.J. Dodson, R. Madupu, L.M. Brinkac, S.C. Daugherty, R.T. DeBoy, A.S. Durkin, M. Gwinn, J.F. Kolonay, S.A. Sullivan, D.H. Haft, J. Selengut, T.M. Davidsen, N. Zafar, O. White, B. Tran, C. Romero, H.A. Forberger, J. Weidman, H. Khouri, T.V. Feldblyum, T.R. Utterback, S.E. Van Aken, D.R. Lovley, C.M. Fraser, Genome of *Geobacter sulfurreducens*: metal reduction in subsurface environments, Science 302 (2003) 1967–1969.
[8] M.V. Coppi, C. Leang, S.J. Sandler, D.R. Lovley, Development of a genetic system for *Geobacter sulfurreducens*, Appl. Environ. Microbiol. 67 (2001) 3180–3187.
[9] Y.H. Ding, K.K. Hixson, C.S. Giometti, A. Stanley, A. Esteve-Núñez, T. Khare, S.L. Tollaksen, W. Zhu, J.N. Adkins, M.S. Lipton, R.D. Smith, T. Mester, D.R. Lovley, The proteome of dissimilatory metal-reducing microorganism *Geobacter sulfurreducens* under various growth conditions, Biochim. Biophys. Acta Proteins and Proteomics 1764 (2006) 1198–1206.
[10] T. Mehta, M.V. Coppi, S.E Childers, D.R. Lovley, Outer membrane *c*-type cytochromes required for Fe(III) and Mn(IV) oxide reduction in *Geobacter sulfurreducens*, Appl. Environ. Microbiol. 71 (2005) 8634–8641.
[11] E.S. Shelobolina, M.V. Coppi, A.A. Korenevsky, L.N. Didonato, S.A Sullivan, H. Konishi, H. Xu, C. Leang, J.E. Butler, B.C. Kim, D.R. Lovley, Importance of *c*-type cytochromes for U(VI) reduction by *Geobacter sulfurreducens*, BMC Microbiol. 7 (2007) 16.
[12] L. Shi, T.C. Squier, J.M. Zachara, J.K. Fredrickson, Respiration of metal (hydr)oxides by *Shewanella* and *Geobacter*: a key role for multihaem *c*-type cytochromes, Mol. Microbiol. 65 (2007) 12–20.
[13] A. Esteve-Núñez, J. Sosnik, P. Visconti, D.R. Lovley, Fluorescent properties of *c*-type cytochromes reveal their potential role as an extracytoplasmic electron sink in *Geobacter sulfurreducens*, Environ. Microbiol. 10 (2008) 497–505.
[14] O. Einsle, S. Foerster, K. Mann, G. Fritz, A. Messerschmidt, P.M.H Kroneck, Spectroscopic investigation and determination of reactivity and structure of the tetraheme cytochrome c_3 from *Desulfovibrio desulfuricans* Essex 6, Eur. J. Biochem. 268 (2001) 3028–3035.
[15] P.M. Matias, J. Morais, R. Coelho, M.A. Carrondo, K. Wilson, Z. Dauter, L. Sieker, Cytochrome c_3 from *Desulfovibrio gigas*: crystal structure at 1.8 Å resolution and evidence for a specific calcium-binding site, Protein Sci. 5 (1996) 1342–1354.
[16] J. Morais, P.N. Palma, C. Frazão, J. Caldeira, J. LeGall, I. Moura, J.J.G. Moura, M.A. Carrondo, Structure of the tetraheme cytochrome from *Desulfvibrio desulfuricans* ATCC 27774: X-ray diffraction and electron paramagnetic resonance studies, Biochemistry 34 (1995) 12830–12841.
[17] M. Czjzek, F. Payan, F. Guerlesquin, M. Bruschi, R. Haser, Crystal structure of cytochrome c_3 from *Desulfovibrio desulfuricans* Norway at 1.7 Å resolution, J. Mol. Biol. 243 (1994) 653–667.
[18] P.M. Matias, C. Frazao, J. Morais, M. Coll, M.A. Carrondo, Structure analysis of cytochrome c_3 from *Desulfovibrio vulgaris* Hildenborough at 1.9 Å resolution, J. Mol. Biol. 234 (1993) 680–699.
[19] M. Assfalg, L. Banci, I. Bertini, M. Bruschi, P. Turano, 800 MHz 1 H NMR solution structure refinement of oxidized cytochrome c_7 from *Desulfuromonas acetoxidans*, Eur. J. Biochem. 256 (1998) 261–270.
[20] M. Assfalg, L. Banci, I. Bertini, M. Bruschi, M.T. Giudici-Orticoni, P. Turano, A proton-NMR investigation of the fully reduced cytochrome c_7 from *Desulfuromonas acetoxidans*: comparison between the reduced and the oxidized forms, Eur. J. Biochem. 266 (1999) 634–643.
[21] M. Czjzek, P. Arnoux, R. Haser, W. Shepard, Structure of cytochrome c_7 from *Desulfuromonas acetoxidans* at 1.9 Å resolution, Acta Crystallogr. D57 (2001) 670–678.
[22] J.R. Lloyd, C. Leang, A.L. Hodges Myerson, M.V. Coppi, S. Cuifo, M. Methe, S.J. Sandler, D.R. Lovley, Biochemical and genetic characterization of PpcA, a periplasmic *c*-type cytochrome in *Geobacter sulfurreducens*, Biochem. J. 369 (2003) 153–161.
[23] L. DiDonato, E. Shelobolina, S. Sullivan, K.P. Nevin, T. Woodward, D.R. Lovley, Characterization of a family of small periplasmic *c*-type cytochromes in *Geobacter sulfurreducens* and their role in Fe(III) respiration, Am. Soc. Microbiol. (2004) General Meeting Abstract.
[24] L. DiDonato, R. DiDonato, B. Postier, B.-C. Kim, D.R. Lovley, Adaption to the loss of periplasmic c_7 cytochromes involved in Fe(III) reduction in *Geobacter sulfurreducens*, Am. Soc. Microbiol. (2006) General Meeting Abstract.
[25] Y.Y. Londer, P.R. Pokkuluri, D.M. Tiede, M. Schiffer, Production and preliminary characterization of a recombinant triheme cytochrome c_7 from *Geobacter sulfurreducens* in *Escherichia coli*, Biochim. Biophys. Acta 1554 (2002) 202–211.
[26] P.R. Pokkuluri, Y.Y. Londer, N.E.C. Duke, W.C. Long, M. Schiffer, Family of cytochrome c_7-type proteins from *Geobacter sulfurreducens*: structure of one cytochrome c_7 at 1.45 Å resolution, Biochemistry 43 (2004) 849–859.
[27] P.R. Pokkuluri, Y.Y. Londer, N.E.C. Duke, J. Erickson, M. Pessanha, C.A Salgueiro, M. Schiffer, Structure of a novel c_7-type three-heme cytochrome domain from a multi-domain cytochrome *c* polymer, Protein Sci. 13 (2004) 1684–1692.
[28] Y.Y. Londer, P.R. Pokkuluri, J. Erickson, V. Orshonsky, M. Schiffer, Heterologous expression of hexaheme fragments of a multidomain cytochrome from *Geobacter sulfurreducens* representing a novel class of cytochromes *c*, Protein Expr. Purif. 39 (2005) 254–260.
[29] Y.Y. Londer, P.R. Pokkuluri, V. Orshonsky, L. Orshonsky, M. Schiffer, Heterologous expression of dodecaheme "nanowire" cytochromes *c* from *Geobacter sulfurreducens*, Protein Expr. Purif. 47 (2006) 241–248.
[30] M. Pessanha, L. Morgado, R.O. Louro, Y.Y. Londer, P.R. Pokkuluri, M. Schiffer, C.A. Salgueiro, Thermodynamic characterization of triheme cytochrome PpcA from *Geobacter sulfurreducens*: evidence for a role played in e^-/H^+ energy transduction, Biochemistry 45 (2006) 13910–13917.
[31] L. Morgado, M. Bruix, V. Orshonsky, Y.Y. Londer, N.E.C. Duke, X. Yang, P.R. Pokkuluri, M. Schiffer, C.A. Salgueiro, Structural insights into the modulation of the redox properties of two *Geobacter sulfurreducens* homologous triheme cytochromes, Biochim. Biophys. Acta 1777 (2008) 1157–1165.
[32] E.H. Gordon, E. Steensma, S.J. Ferguson, The cytochrome *c* domain of dimeric cytochrome cd_1 of *Paracoccus pantotrophus* can be produced at high levels as a monomeric holoprotein using an improved *c*-type cytochrome expression system in *Escherichia coli*, Biochem. Biophys. Res. Commun. 281 (2001) 788–794.
[33] J. Sambrook, E.F. Fritsch, T. Maniatis, Molecular Cloning: A Laboratory Manual, Cold Spring Harbor Laboratory Press, New York, 1989.
[34] E. Arslan, H. Schulz, R. Zufferey, P. Kunzler, L. Thöny-Meyer, Overproduction of the *Bradyrhizobium japonicum c*-type cytochrome subunits of the *cbb*3 oxidase in *Escherichia coli*, Biochem. Biophys. Res. Commun. 251 (1998) 744–747.

[35] Z. Otwinowski, W. Minor, Processing of x-ray diffraction data collected in oscillation mode, Methods Enzymol. 276 (1997) 307–326.
[36] A.T. Brünger, P.D. Adams, G.M. Clore, W.L. Delano, P. Gros, R.W. Grosse-Kunstleve, J.-S. Jiang, J. Kuszewski, M. Nigles, N.S. Pannu, R.J. Read, L.M Rice, T. Simonson, G.L. Warren, Crystallography and NMR system: a new software suite for macromolecular structure determination, Acta Crystallogr. D54 (1998) 905–921.
[37] J.S. Sack, CHAIN—A crystallographic modeling program, . Mol. Graphics 6 (1988) 224–225.
[38] G.N. Murshudov, A.A. Vagin, A. Lebedev, K.S. Wilson, E.J. Dodson, Efficient anisotropic refinement of macromolecular structures using FFT, Acta Crystallogr. D Biol. Crystallogr. 55 (1999) 247–255.
[39] A. Dolla, L. Florens, M. Bruschi, I.V. Dudich, A.A. Makarov, Drastic influence of single heme axial ligand replacement on the thermostability of cytochrome c_3, Biochem. Biophys. Res. Commun. 211 (1995) 742–747.
[40] W. Jentzen, J.-G. Ma, J.A. Shelnutt, Conservation of the conformation of the porphyrin macrocycle in hemoproteins, Biophys. J. 74 (1998) 753–763.
[41] E. Krissinel, K. Henrick, Inference of macromolecular assemblies from crystalline state, J. Mol. Biol. 372 (2007) 774–797.
[42] A. Nicholls, K.A. Sharp, B. Honig, Protein folding and association: insights from the interfacial and thermodynamic properties of hydrocarbons, Proteins 11 (1991) 282–296.
[43] L. Pieulle, X. Morelli, P. Gallice, E. Lojou, P. Barbier, M. Czjzek, P. Bianco, F. Guerlesquin, E.C. Hatchikian, The type I/type II cytochrome c_3 complex: an electron transfer link in the hydrogen-sulfate reduction pathway, J. Mol. Biol. 354 (2005) 73–90.
[44] N. Yahata, T. Saitoh, Y. Takayama, K. Ozawa, H. Ogata, Y. Higuchi, H. Akutsu, Redox interaction of cytochrome c_3 with [NiFe] hydrogenase from *Desulfovibrio vulgaris* Miyazaki F, Biochemistry 45 (2006) 1653–1662.
[45] L. El Antak, X. Morelli, O. Bornet, C. Hatchikian, M. Czjzek, A. Doll, F. Guerlesquin, The cytochrome c_3-[Fe]-hydrogenase electron transfer complex: structural model by NMR restrained docking, FEBS Lett. 548 (2003) 1–4.
[46] Y-H.R. Ding, K.K. Hixson, M.A. Aklujkar, M.S. Lipton, R.D. Smith, D.R. Lovley, T. Mester, Proteome of *Geobacter sulfurreducens* grown with Fe(III) oxide or Fe(III) citrate as the electron acceptor, Biochim. Biophys. Acta Proteins and Proteomics 1784 (2008) 1935–1941.